ZERO-DIMENSIONAL MODEL FOR A 4-STROKE, DIRECT INJECTION, VARIABLE COMPRESSION RATIO FOR MAXIMUM TORQUE

Abou Al-Sood M.M. *, Abdel-Rahim, Y. M. and Ahmed, M. A.
*Author for correspondence
Department of Mechanical Engineering,
Assiut University,
Assiut, 71516,
Egypt,
E-mail: m_aboualsood@hotmail.com

ABSTRACT

A zero-dimensional model for simulation the performance of a four-stroke direct-injection (DI) diesel engine is developed. The simulation model includes detailed sub-models for fuel burning rate, combustion products, thermodynamic properties of working fluid, heat transfer, fluid flow, and both soot and NO_x formation mechanisms. To validate the model, comparisons between experimental and predicted results for different engines, operating under different conditions were conducted. Comparisons show that there is a good concurrence between measured and predicted values. An optimization analysis is conducted for seeking an optimum variation of compression ratio to achieve pre-set objective target of constant maximum brake torque. The optimization analysis is performed under the constrain that the maximum pressure and temperature inside the cylinder not exceed the maximum allowable pressure and temperature of the conventional engine (constant compression ratio, r_c).Varying compression ratio is optimized with the previous condition. Results indicated that optimum brake torque is achieved when the value of, r_c, ranged between 16.4 and 19.3, where the brake specific fuel consumption, bsfc, and soot emission are reduced by about 4.6% and 12 %, respectively. Furthermore, the brake torque is increases by about 5.4%; NO_x, maximum pressure (p_{max}) , and maximum temperature (T_{max}) are increased by about 90.7 %, 10.3% and 3.6 %, respectively.

INTRODUCTION

Requirements to provide environmental friendly vehicles (i.e. low fuel consumption with less emission) have resulted in using the most complicated and intellectual means of internal combustion engine development. Nowadays new ideas, which could not be discussed two decades ago, are being considered by automotive manufacturers. In particular, many leading automotive companies have approached practically the very complicated design ideas with different aspects of diesel/petrol engine design. These aspects have been under extensive theoretical and experimental investigations. The most important aspect of design is aimed to vary the engine compression ratio (r_c) depending on load, or speed, or both load and speed. Several trials have been done in that respect with extensive design, experimentation and measurements [1-6]. All attempts to change the compression ratio are achieved by one or more of the following concepts [1]: (1) moving the cylinder head, (2) variation of combustion chamber volume, (3) variation of piston deck height, (4) modification of connecting rod geometry (usually by means of some intermediate member), (5) moving the crankpin within the crankshaft (effectively varying the stroke), and (6) moving the crankshaft axis.

Variable-stroke engine mechanism patented by Freudenstein and Maki [2] was used by Yamin and Dado [3] as it gives availability to change the stroke length and the corresponding compression ratio in the range of 6.82 to 10. Their results showed a significant improvement in the engine's power, and reduction in the fuel consumption. In addition to an increase in Carbon monoxide (CO) and Nitric oxides (NO_x) compared with the actual engine. Finally, they concluded that the engine performance can be optimized for a full range of driving conditions, such as acceleration, speed and load. Such optimized performance was obtained by incorporating some means to suppress the increase in emissions rate to be applicable in the automotive field due to the strict anti-pollution laws.

Befits and challenges of Variable Compression Ratio (VCR) spark ignition engines had been illustrated, examined and critically reviewed by Roberts [1]. Also, the implications for volume manufacture and the strategy for VCR implementation in order to produce the maximum benefit had been discussed. Ladommatos and Balian [4] studied the effects of an increased clearance volume on the performance of a direct-injection diesel engine. This study was conducted to overcome problems

with combustion at conventional compression ratio, i.e. constant r_c, and at variable r_c, but lower that the conventional r_c. Rychter et *al.* [5] evaluated the concept of varying r_c to give different expansion and compression ratios by means of a theoretical simulation of a turbocharged diesel engine. They varied the ratio of connecting rod length to crank throw to study the effect of r_c on engine performance at a fixed load. The principal benefits, at 3/4 load and compression ratio of 20, were a reduction in fuel consumption by about 2 % and a reduction in ignition delay that leads to an estimated 6 dB reduction in combustion noise.

Sobotowski et *al.* [6] modified a prototype direct injection diesel engine to incorporate BP Oil variable compression ratio (VCR) engine concept. Their objective was achieved by altering the phase relation between two pistons linked to separate crankshafts and operating in two cylinders arranged in an opposed engine or interconnected through a transfer port. According to their concept, a novel crankshaft phasing mechanism was employed to achieve r_c variation with a number of significant advantages over other VCR engine designs. These advantages includes: (a) mechanical simplicity and compact design, (b) capability to externally control r_c during engine operation, (c) automatic variation of valve timing and, (d) compatibility with current production technology.

Thermodynamic models (zero-dimensional), and turbulent models (multi-dimensional) are commonly used in internal combustion engines modeling. The first one, which are mainly based on the energy conservation (first law of thermodynamics), have shown a good agreement with real engine trends (e.g. [7-9]). On the other hand, models of the second one (e.g. [10-15]), are less phenomenological than the first one due to their need to many empirical sub-models for their completion and its time consuming for execution.

The purpose of this study is to develop a simple, rapid, and accurate simulation model based on thermodynamic analysis without the need for a great deal of computational power or knowledge of precise engine geometrical data to predict the range of compression ratio corresponding to the optimum engine performance (brake specific fuel consumption (bsfc), and brake torque). The developed model is based on mass and energy conservation laws, equation of state, heat transfer between the working fluid and cylinder walls, fuel energy release rate, and engine friction losses. Single zone combustion is assumed, and thermodynamic properties are calculated from chemical equilibrium principles for six and/or eleven species. A stepwise solution is carried out for varying compression ratio and the engine speed over its entire range (i.e., 1500 rpm to 2800 rpm). In calculations, the temperature and pressure cannot exceed the maximum allowable temperature and pressure of the conventional engine, at a constant compression ratio, which are 2100 K and 10.7 MPa, respectively.

NOMENCLATURE

Symbols

CN	[--]	fuel Cetane Number
c_p, c_v	[J/kg.k]	constant pressure and volume specific heats (J/kg.K)
D_{iv}	[m]	intake valve head diameter (m)
h	[J/kg]	enthalpy (J) , and specific enthalphy (J/kg)
k	[--]	specific heat ratio
m	[kg]	mass (kg)
N	[rpm]	crank speed (rpm)
n	[kmol]	number of moles (mole)
n_c	[--]	number of cylinders per engine
n_{iv}, n_r	[--]	number of intake valves, and rings per cylinder
p	[N/m^2]	pressure (Pa)
Q, q	[J, J/m^2]	heat transfer (J), and heat flux (J/m^2)
r_c	[--]	compression ratio
R	[J/kg.K]	gas constant (J/kg.k)
S_p	[m/s]	mean piston velocity (m/s)
T	[K]	cylinder temperature (K)
V, V_c, V_d	[m^3]	swept; clearance and maximum displacement volumes (m^3)
X	[--]	Mole fraction

Greek symbols

θ	degree]	crank position angle (degrees)
λ	[--]	connecting rod length to crank radius ratio
$\theta_{evo}, \theta_{ivo}$	[degree]	exhaust and intake valves opening angles (degrees)
$\Delta\theta_{eopen}$	[degree]	opening duration angle of exhaust valve (degree)
$\Delta\theta_{iopen}$	[degree]	opening duration angle of intake valve (degree)
ρ	[kg.m^3]	density (kg/m^3)
ϕ	[--]	equivalence ratio
$\tau, \bar{\tau}$	[degree]	ignition delay period (milliseconds) and ignition delay angle (degrees)

Abbriviation

gm	grams
w.r.t	**with respect to**

Subscripts

b	backward
comb	combustion
e	exit; equilibrium
em	exhaust manifold
ex	exhaust
f	fuel; forward
fb	fuel burning
ft	total fuel
i	indicated; inlet; injection start
ig	ignition
im	intake manifold
In	intake
o	ambient condition
p	piston
s	Stoichiometry, soot
sf, so	soot formation and soot oxidation
w	Wall, atoms of carbon in fuel-air molecule
x	hydrogen atoms in fuel-air molecule
y	oxygen atoms in fuel-air molecule
z	nitrogen atoms in fuel-air molecule

Superscripts

.	derivative with time (d/dt)
-	molar quantity

MATHEMATICAL MODEL

Over the past few decades there have been a substantial progress in the ability to model actual processes that occur inside the cylinder of the diesel engine. The purpose of the present study is to utilize thermodynamics, heat transfer, fluid mechanics, and chemical kinetics fundamentals to predict the operating characteristics of four-stroke, direct-injection diesel engine with variable compression ratio. To achieve this goal, separate sub-models representing different engine aspects are

integrated in the main engine simulation model. These sub-models are: engine geometry, combustion products, thermodynamic properties, engine friction and heat transfer, mass exchange, combustion rate, temperature-pressure and emission mechanisms. These models are applied to the different processes of actual cycle of a direct-injection diesel engine and their corresponding governing equations are solved numerically by constructing a FORTRAN computer code. The main assumptions considered in this numerical investigation are as follows: (*i*) the content of the cylinder is a homogeneous gas mixture of air (79% N_2 and 21% O_2 by volume), where fuel vapor and combustion products and its thermodynamic properties are calculated using ideal gas laws with temperature dependent specific heats, (*ii*) pressure and temperature inside the cylinder are uniform and vary with the crank angle, (*iii*) the gas motion inside the cylinder (created by pressure gradients due to piston motion) is neglected, (*iv*) single zone combustion process starts from a rapid premixed burning phase, followed by slower mixing controlled burning phase and, (*v*) temperatures of the cylinder head, cylinder walls and piston crown are assigned constant values. The detail of the numerical models is outlined below.

A. Engine Geometry:

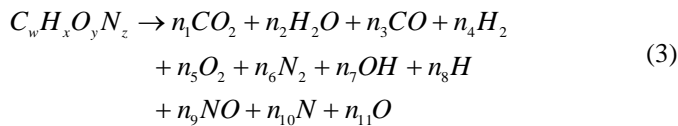The rate of change of the volume with respect to time is given as:

$$\dot{V} = V_c \left[\frac{r_c - 1}{2} \sin\theta \frac{1 + \cos\theta}{\sqrt{\lambda^2 - \sin^2\theta}} \dot{\theta} \right] \tag{1}$$

B. Combustion Products Model

For temperature < 1600 K. the equilibrium composition of gases produced by the combustion of a general hydrocarbon fuel with air (having a general fuel-air molecule in the form $C_w H_x O_y N_z$) is calculated based on the assumption that only gaseous phases are considered. The general combustion equation of the fuel in air can be written as:

$$C_w H_x O_y N_z \rightarrow n_1 CO_2 + n_2 H_2O + n_3 CO + n_4 H_2 \\ + n_5 O_2 + n_6 N_2 \tag{2}$$
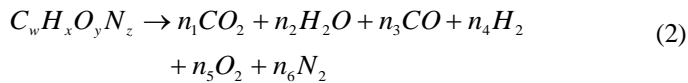
For temperature $\geq$ 1600 K, eleven combustion products are assumed. The chemical reaction can be written as:

$$C_w H_x O_y N_z \rightarrow n_1 CO_2 + n_2 H_2O + n_3 CO + n_4 H_2 \\ + n_5 O_2 + n_6 N_2 + n_7 OH + n_8 H \\ + n_9 NO + n_{10} N + n_{11} O \tag{3}$$

Obtaining moles of eleven combustion products, eleven equations are needed (i.e. four equations from mass balance of C, H, O, and N in (3), and seven equations from chemical equilibrium). These equations have been solved by procedure mentioned in [16].

C. Thermodynamic Properties of Cylinder Content Model

During each thermal cycle, the cylinder contains in general, air, fuel vapor, and combustion products with different proportions depending on the engine conditions under consideration. The specific heat under constant pressure, enthalpy, and entropy of the cylinder content are given by:

$$\bar{c}_p = \sum_{i=1}^{zz} X_i \bar{C}_{p_i}, \quad \bar{h} = \sum_{i=1}^{zz} X_i \bar{h}_i \tag{4}$$

where $X_i = n_i / \sum_{i=1}^{zz} n_i$, and zz (number of different gases) = 6, and 11 for T<1600 K, and $T \geq$ 1600 K, respectively.

D. Engine Friction Model

Empirical correlations of losses are in terms of compression ratio, engine speed, bore, stroke, intake and exhaust manifold pressures, and valves geometry [17] are used in this work. These correlations were concluded to the following friction categories as follows:

(i) Piston losses:
$$(fmep)_p = 6.2n_r + \left[0.606\,r_c + 1.254\,r_c^{1.37-0.0238S_P}\right] + 9.3S_P^{1.03} \tag{5}$$
(ii) Blowby losses:
$$(fmep)_b = 11.86r_C^{0.4} - (3.38 + 0.103r_c) \\ + 6.89[N/1000]^{1.185} \tag{6}$$
(iii) Exhaust and inlet system throttling losses:
$$(fmep)_{ei} = P_{im} + P_{em}/2.75 \tag{7}$$
(iv) Crankcase mechanical losses:
$$(fmep)_c = 12.122\left(\frac{dN}{1000\,L}\right) + \\ + 0.07\left[30 - \left(\frac{4N}{1000}\right)\right]\left[\frac{n_{iv}D_{iv}^{1.75}}{d^2 L}\right] \\ + 2.688\left(\frac{N}{1000}\right)^{1.5} \tag{8}$$
(v) Combustion chamber and valve pumping losses:
$$(fmep)_{CC} = 8.96(N/1000)^{1.7} \times \left[2.98V_d/n_{iv}\,n_c\,D_{iv}^2\right]^{1.298} \tag{9}$$

The intake and exhaust manifold gage pressures (p_{im}, p_{em}) in (7) are taken as reported by [18] as: $p_{im} = 0$, $p_{em} = 0.062(N/1000)^2$.

The overall engine frictional power losses are obtained by:
$$(fmep)_{overall} = V_d(N/120)n_c \sum_{i=1}^{5}(fmep)_i \tag{10}$$

E. Engine Heat Transfer Model

Eichelberg [19] derived a simple equation for calculating the instantaneous heat flux out of the engine $\dot{q}_w$ in (W/m²) in terms of cylinder temperature, pressure, and piston mean velocity. Rakopoulos and Hountalas [20] modified this equation into the form:

$$\dot{q}_w = 1.99(S_p)^{1/3}(pT)^{1/2}(T-T_w) \tag{11}$$

Radiation heat transfer was neglected in some studies such as (e.g. [21- 23]), but it had been considered in others (e.g. [24-26]). In the present simulation the Eichelberg [19] model as modified by Rakopoulos and Hountalas [20] is used with the values of piston crown, cylinder head, and cylinder wall temperatures are taken to be 610 K, 510 K, 510 K, respectively.

F. Mass Exchange Model

Air Intake and Exhaust Exchange- The mass flow rates through the valves are usually described by the equation for compressible, one-dimensional isentropic flow. The real flow effects are included by means of an experimentally determined discharge coefficient. In the present simulation, the discharge coefficient is taken as reported in [27] and equal to $\sin[\pi(\theta-\theta_{vo})/\Delta\theta_{open}]^{1/3}$. The gas flow rate is related to the upstream stagnation pressure, stagnation temperature, and static pressure just downstream of the flow restriction. For the flow into cylinder through intake valve, the upstream stagnation pressure and temperature are the intake manifold pressure and temperature (p_{im}, T_{im}), and downstream static pressure is the cylinder pressure (p). For flow out of the cylinder through exhaust valve, the upstream stagnation pressure and temperature are the cylinder pressure and temperature (p, T), and downstream static pressure is the exhaust manifold pressure (p_{em}) [27, 28]. The mass flow rates entering and leaving the cylinder are defined as follows [29]:

For subsonic inflow where $\dfrac{p}{p_{in}} < \left(\dfrac{2}{k+1}\right)^{\frac{k}{k-1}}$:

$$\dot{m}_{in} = A_{in}p_{im}\sqrt{\left(\frac{2k}{(k-1)RT_{im}}\right)\left(\frac{p}{p_{im}}\right)^{\frac{2}{k}}\left(1-\left(\frac{p}{p_{im}}\right)^{\frac{k-1}{k}}\right)} \tag{12}$$

For sonic and supersonic inflow where $\dfrac{p}{p_{in}} \geq \left(\dfrac{2}{k+1}\right)^{\frac{k}{k-1}}$:

$$\dot{m}_{in} = A_{in}p_{im}\sqrt{\left(\frac{k}{RT_{im}}\right)\left(\left(\frac{2}{k+1}\right)^{\frac{k+1}{k-1}}\right)} \tag{13}$$

For subsonic outflow where $\dfrac{p}{p_{em}} < \left(\dfrac{2}{k+1}\right)^{\frac{k}{k-1}}$:

$$\dot{m}_{ex} = A_{ex}p\sqrt{\left(\frac{2k}{(k-1)RT}\right)\left(\frac{p_{em}}{p}\right)^{\frac{2}{k}}\left(1-\left(\frac{p_{em}}{p}\right)^{\frac{k-1}{k}}\right)} \tag{14}$$

For sonic and supersonic outflow where $\dfrac{p_{em}}{p} \geq \left(\dfrac{2}{k+1}\right)^{\frac{k}{k-1}}$

$$\dot{m}_{ex} = A_{ex}p\sqrt{\left(\frac{k}{RT}\right)\left(\left(\frac{2}{k+1}\right)^{\frac{k+1}{k-1}}\right)} \tag{15}$$

where k is the specific heat ratio and its value are taken as the ratio of specific heats (c_p/c_v) of the cylinder contents

Mass of Injected Fuel- Mass of fuel injected into cylinder m_f (relative to total injected mass m_{ft}) is written (according to [30, 31]) in terms of crank angle (θ) as follows:

$$\left(\frac{m_f}{m_{ft}}\right) = \frac{1}{2}\left\{1-\cos\left(\frac{\pi(\theta-\theta_o)}{\Delta\theta_{injection}}\right)\right\} \tag{16}$$

Differentiation of the above equation w.r.t. time leads to the following equation:

$$\left(\frac{\dot{m}_f}{m_{ft}}\right) = \left(\frac{\pi}{2\Delta\theta_{injection}}\right)\sin\left(\frac{\pi(\theta-\theta_o)}{\Delta\theta_{injection}}\right)\dot{\theta} \tag{17}$$

G. Combustion Rate Model

Watson *et al.* [32] developed equations for fuel energy release appropriate for diesel engine simulations. In their development, the combustion process starts from a rapid premixed burning phase (represented by function f_1), followed by a slower mixing controlled burning phase (represented by function f_2), with both functions are empirically linked to the duration of ignition delay ($\tilde{\tau}_{id}$) and the duration of combustion ($\Delta\theta_{comb}$). According to their model, the burned mass of fuel at any angle (θ) related to total injected mass (m_{ft}) is:

$$m_{fb}(\hat{\theta})/m_{ft} = \beta f_1 + (1-\beta)f_2 \tag{18}$$

where:

$f_1 = 1-(1-\hat{\theta}^k)^k$, $\hat{\theta} = (\theta-\theta_{ig})/\Delta\theta_{comb}$, and $\beta = 1-0.92\phi^{0.37}\tau_{id}^{-0.26}$

The ignition delay ($\tilde{\tau}_{id}$) is calculated in degrees of crank angle by empirical correlations [28, 33]. These correlations are in terms of intake manifold temperature T_{im} (in Kelvin) and pressure p_{im} (in bars), compression ratio r_c, fuel Cetane Number (CN)), and mean piston velocity S_p (m/s) as follows:

$$\tilde{\tau}_{id} = (0.36+0.622S_p)\exp\left[\left(\frac{618840}{CN+25}\right)\times\right. \tag{19}$$
$$\left.\left(\frac{1}{RT_{im}r_c^{k-1}}-\frac{1}{17190}\right)\times\left(\frac{21.2}{P_{im}r_c^k-12.4}\right)^{0.63}\right]$$

The ignition delay period can be expressed in milliseconds according to $\tau_{id} = [\tilde{\tau}_{id}/0.006N]$. Values of the empirical coefficients k_1, k_2, k_3 and k_4 are reported in [28, 34] as follows:
$k_1 = 2+1.25*10^{-8}(\tau_{id}/N)^{2.4}$, $k_2 = 5000$, $k_3 = (14.2/\phi^{0.644})$,
and $k_4 = 0.79k_3^{0.25}$. The fuel burning rate w.r.t crank angle (θ) can be obtained by differentiating (18) as follows:

$$\left(\frac{dm_{fb}}{d\theta}\right) = m_{ft}\frac{\beta k_1 k_2(1-\hat{\theta}^{k_1})^{(k_2-1)}\hat{\theta}^{(k_1-1)}+k_3k_4(1-\beta)\hat{\theta}^{(k_4-1)}\exp(-k_3\hat{\theta}^{k_4})}{\Delta\theta_{comb}}$$
$$\tag{20}$$

H. Temperature - Pressure Relationships

The changes of pressure and temperature with respect to time are defined as follows:

$$\dot{P} = \frac{\rho}{\partial\rho/\partial P}\left(-\frac{\dot{V}}{V} - \frac{\dot{T}}{\rho}\frac{\partial\rho}{\partial T} - \frac{\dot{\phi}}{\rho}\frac{\partial\rho}{\partial\phi} + \frac{\dot{m}}{m}\right) \qquad (21)$$

$$\dot{T} = \frac{B^{\circ}}{A^{\circ}}\left\{-\frac{\dot{V}}{V} + \left(1 - \frac{h}{B^{\circ}}\right)\frac{\dot{m}}{m} - \frac{C^{\circ}}{B^{\circ}}\dot{\phi} + \frac{1}{mB^{\circ}}\left(\sum_{j}\dot{m}_{j}h_{j} + \dot{Q}_{w}\right)\right\} \qquad (22)$$

where $A^{\circ} = \left(\frac{\partial h}{\partial T}\right) + \frac{(\partial\rho/\partial T)}{(\partial\rho/\partial P)}\left(\frac{1}{\rho} - \frac{\partial h}{\partial P}\right)$, $B^{\circ} = \frac{1 - \rho(\partial h/\partial P)}{(\partial\rho/\partial P)}$, and

$$C^{\circ} = \frac{\partial h}{\partial\phi} + \frac{(\partial\rho/\partial\phi)}{(\partial\rho/\partial P)}\left(\frac{1}{\rho} - \frac{\partial h}{\partial P}\right)$$

I. Soot Mechanism

Hiroyasu and Kadota. [35] developed a simple soot model to predict the production rate of soot mass ($\dot{m}_{s}$) using a single-step competition between the soot mass formation rate $\dot{m}_{sf}$ and the soot mass oxidation rate $\dot{m}_{so}$ according to: $\dot{m}_{s} = \dot{m}_{sf} - \dot{m}_{so}$. Morel et al. [36] and Wahiduzzaman et al. [37] suggested models for soot formation and their oxidation in diesel engines. In their models, the time rates of soot formation and oxidation are given by:

$$\dot{m}_{sf} = 0.3m_{fb}\exp\left(-\frac{3000}{T_{af}}\right)\dot{\theta} \qquad (23)$$

$$\dot{m}_{so} = \left(\frac{0.4m_{s}\exp\left(-\frac{10000}{T}\right)\sqrt{p_{O_2}}}{6\rho_{s}d_{s}N}\right)\dot{\theta} \qquad (24)$$

where m_{fb} is the mass of fuel burned,
T_{af} is the adiabatic flame temperature at equivalence ratio of 1.1, d_{s} (the soot particle diameter) = 0.022×10^{-6} m , ρ_{s} (soot density) = 1800 kg/m^3 [38].

J. NOx Mechanism

The extended Zeldovich mechanism for NOx formation rate [27] is formed as follows:

$$\frac{d}{dt}[NO] = 2k_{1f}[O]_{e}[N_{2}]_{e}\left(\frac{1 - [NO]^{2}/K_{12}[O_{2}]_{e}[N_{2}]_{e}}{1 + k_{1b}[NO]/(k_{2f}[O_{2}]_{e} + k_{3f}[OH])_{e}}\right) \qquad (25)$$

Where: $K_{12} = (k_{1f}/k_{1b})/(k_{2f}/k_{2b})$, The constants above are taken as follow: $k_{1f} = 7.6 \times 10^{13}\exp\left(-\frac{38000}{T}\right)$,

$k_{2f} = 6.4 \times 10^{9}T\exp\left(-\frac{3150}{T}\right)$, $k_{3f} = 4.1 \times 10^{13}$, $k_{1b} = 1.6 \times 10^{13}$,

and $k_{2b} = 1.5 \times 10^{9}T\exp\left(-\frac{19500}{T}\right)$.

SOLUTION PROCEDURE

The governing equations (1-25) of the comprehensive model subjected to the assumptions previously mentioned in mathematical model are solved for different processes of the engine cycle. The fourth order Rung-Kutta method is used to simulate the comprehensive model equations at the prescribed initial conditions. The engine cycle starts from the moment the exhaust valve closes. Solution is carried out with end results of each process taken as the starting conditions for the following

process, and end values for the completed thermal cycle taken as the starting values for the subsequent cycle. The solution is iterated and considered satisfactory when the end values of temperature and pressure of the cycle are within ± 0.001 % from the starting values of temperature and pressure of the same cycle. Inputs to the code are the engine specifications similar to HELWAAN M114, operating conditions and fuel data listed in Table I. The numerical output results are the instantaneous pressure, temperature, volume, heat transfer, work, mass exchange, fuel heat release, and engine performance variables such as brake specific fuel consumption(bsfc), indicated mean effective pressure (imep), brake mean effective pressure (bmep), indicated power, brake power, and volumetric, indicated, brake and mechanical efficiencies.

Table 1
Engine specifications and operating conditions

Engine type	HELWAAN M114
Cylinder bore	112 mm
Stroke	115 mm
Number of cylinders	4
Intake valve open angle	9 deg. BTDC
Intake valve close angle	43 deg. ABDC
Exhaust valve open angle	40 deg. BBDC
Exhaust valve close angle	12 deg. ATDC
Start of injection	22 deg. BTDC
Number of injector nozzles	1 with 3 holes
Diameter of injector nozzles	0.45 mm
Conventional compression ratio	16.4
Engine speed range	1500- 2800 rpm
Overall equivalence ratio	0.47
Fuel type	$C_{10.8}H_{18.7}$
Lower latent heat of fuel	42MJ/kg

RESULTS AND DISCUSSIONS

Simulation Results

The numerical simulation results are performed for a conventional direct injection (DI) diesel engine with constant compression ratio (specifications and operating conditions are given in Table 1). Sample of these results represent the engine thermodynamic cycle, temperature and pressure variation throughout the cycle, the rates of mass entering and leaving cylinder, and the in-cylinder NOx and soot history along the cycle are displayed in Figures 1 through 4, respectively.
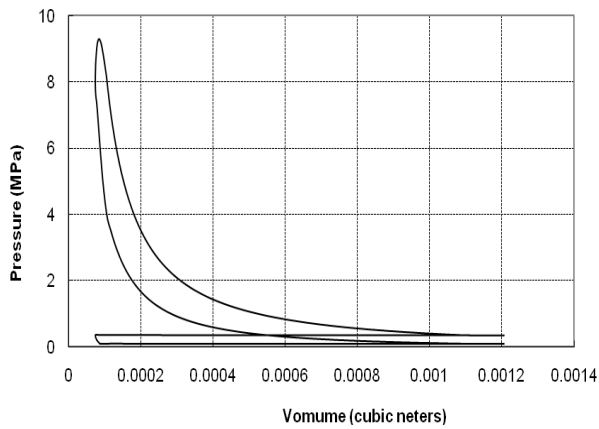
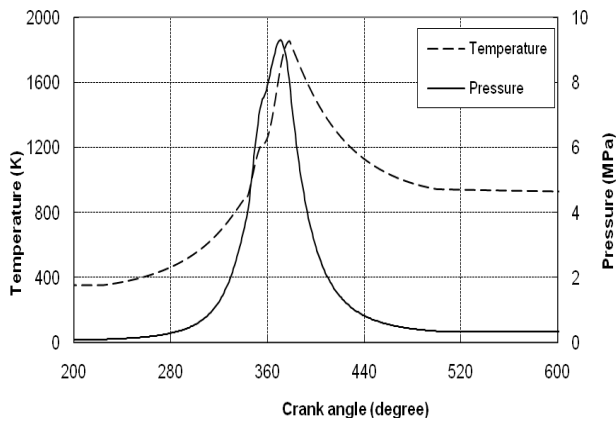**Figure 1** Pressure-volume diagram along engine cycle at 2100 rpm

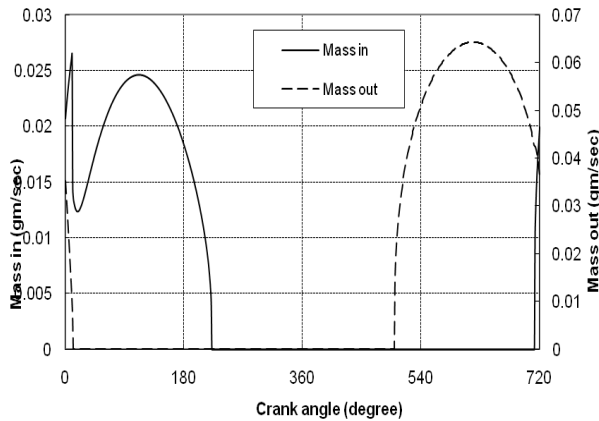**Figure 2** Cylinder pressure and temperature vs. crank angle at 2100 rpm

Figure 3 Instantaneous mass flow rate of air through intake valve and exhaust gases through exhaust valve at 2100 rpm
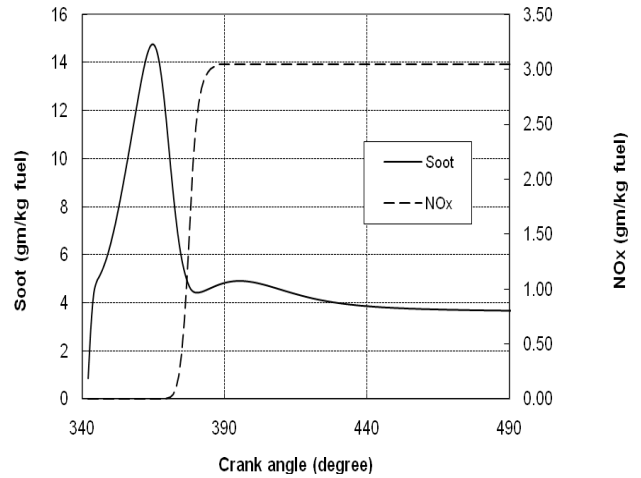

Figure 4 Soot and NO_x inside cylinder of the engine at 2100 rpm

Model Validation

In order to validate the present developed model, comparisons between the numerically results and the available measurements are conducted. Two sets of experimental data reported by [13, 37] are used to validated the developed model as shown in Figures 5-6. Figure 1 shows the comparison between the predicted and measured pressure versus crank angle.
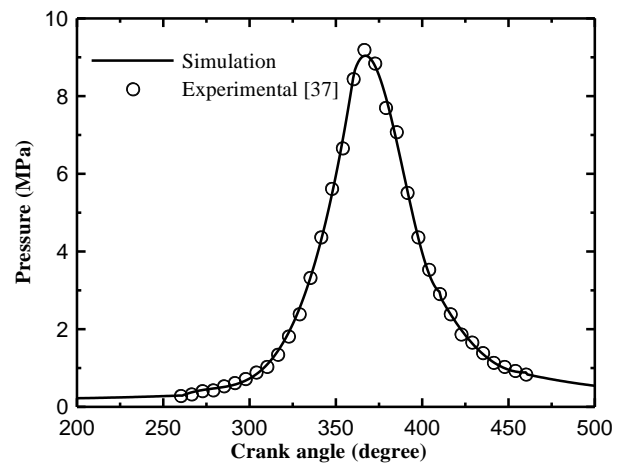
Figure 5 Predicted and measured pressure versus crank angle

Figure 2 presents the comparison between the predicted and measured heat release rate versus crank angle. Based on these

1236

figures, one can observe that there is a good concurrence between measured and predicted results for different engines under different operating conditions.
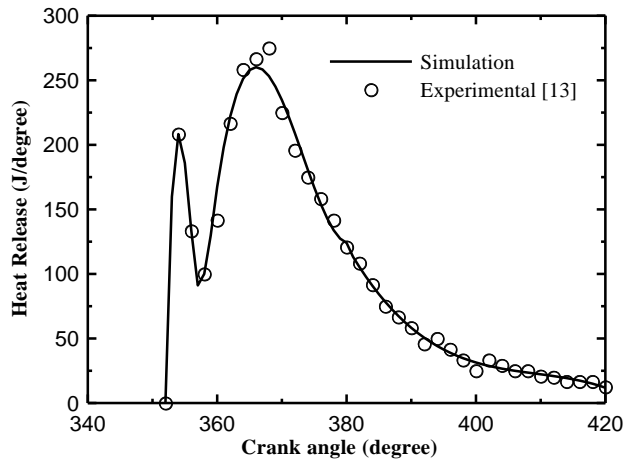

Figure 6 Predicted and measured heat release versus crank angle

Variation of the compression ratio

The numerical simulation results are used to determine the range of compression ratio corresponding to the optimum engine performance for maximum brake torque under the restriction of maximum allowable pressure and temperature. The numerical results of the optimization process, for engine specifications previously mentioned as shown in Table 1, are presented in Figures 7 through 12. It is worth mentioning that for all figures, the solid lines represent performance of optimum variable r_c, while dashed lines represent performance of conventional constant r_c engine.

Figure 7 shows that the brake torque, in case of a constant compression ratio, changes between 281 N.m and 252 N.m passing through a maximum of 295 N.m at about 1900 rpm. For the variable compression ratio, the brake torque is kept constant at its maximum value of 295 N.m over speed ranged from 1500 to 2460 rpm by varying compression ratio between 16.4 and 19.3. This means that the brake torque increases by 5.4 % at 1500 rpm and 4.6 % at 2460 rpm. The shown variation trend in compression ratio urges that actual variation in compression ratio should be considered to increase the brake torque to its constant maximum value.

Figure 8 shows the increase in p_{max} and T_{max} when operating under variable compression ratio *compared* to the operation under constant compression ratio. The increase in p_{max} is about 0.9 MPa at 1500 rpm and 0.6 MPa at 2460 rpm passing through zero MPa at about both

1900 and 2800 rpm. The noticeable increase in T_{max} is about 60 K at 1500 rpm, and 40 K at 2460 rpm passing through zero at both 1900 and 2800 rpm. These increases in p_{max}, and T_{max} are tolerable, as they are still below the allowable pressure and temperature of the conventional engine. Similar observations for the changes of brake efficiency and bsfc versus engine speed for operation under constant and variable compression ratio are shown in Figure 9. If the compression ratio is constant, the brake thermal efficiency varies between 36 % and 32.9 % passing through a maximum value of 37.3 % at engine speed of 1900 rpm. In case of varying compression ratio (between 16.4 and 19.3 for maximum torque), the efficiency changes between 37.6 % at 1500 rpm, and 36.5% at 2460 rpm. In addition to gains in brake torque and efficiency, the figure shows a decrease in the bsfc over engine speed ranging from 4.6 % at 1500 rpm to 2.7 % at 2460 rpm passing through zero % at both 1900 and 2800 rpm.
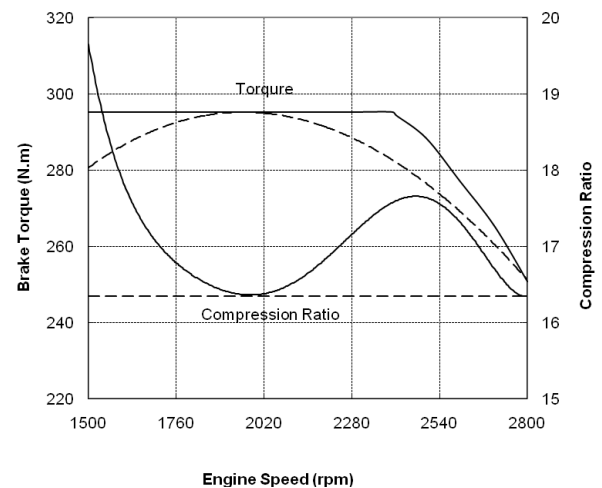

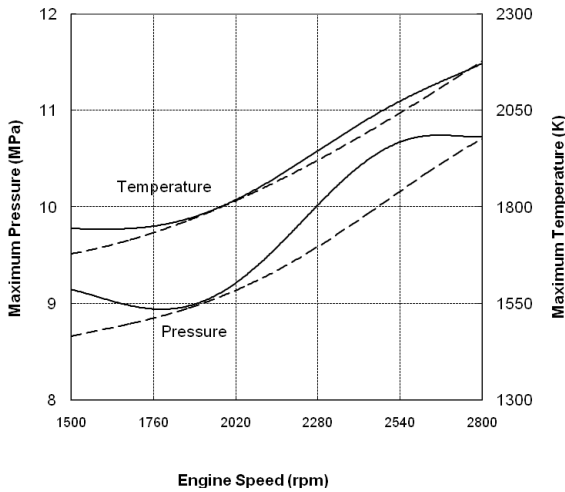**Figure 7** Brake torque and power vs. speed for constant and variable compression ratio engines

Figure 8 Maximum cylinder pressure and temperature vs. speed for constant and variable compression ratio engines

Figure 9 bsfc and thermal efficiency vs. speed for constant and variable compression ratio engines

2800 rpm. Also, this figure shows that variation of the compression ratio for optimum brake torque results in a general decrease in residual gas fraction (RGF) by about 6.5 % at 1500 rpm, and 5 % at 2460 rpm passing through zero % at both 1900 and 2800 rpm.
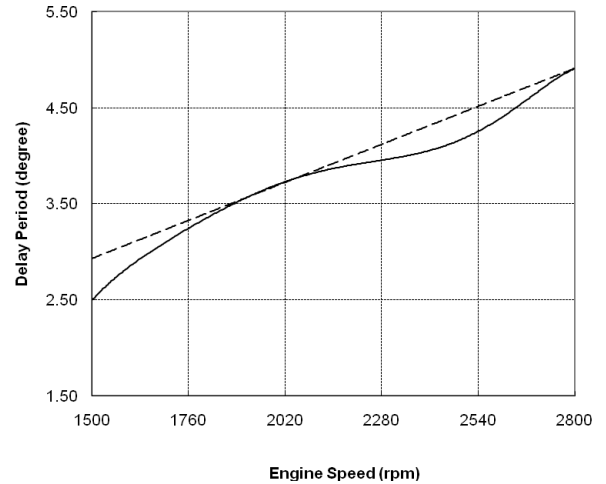

Figure 10 Delay period vs. speed for constant and variable compression ratio engines
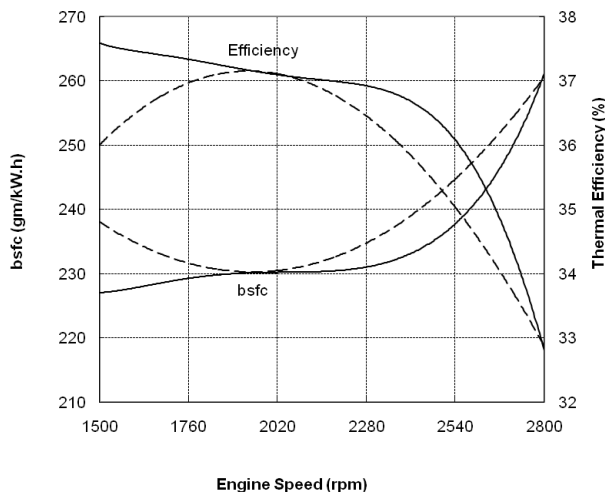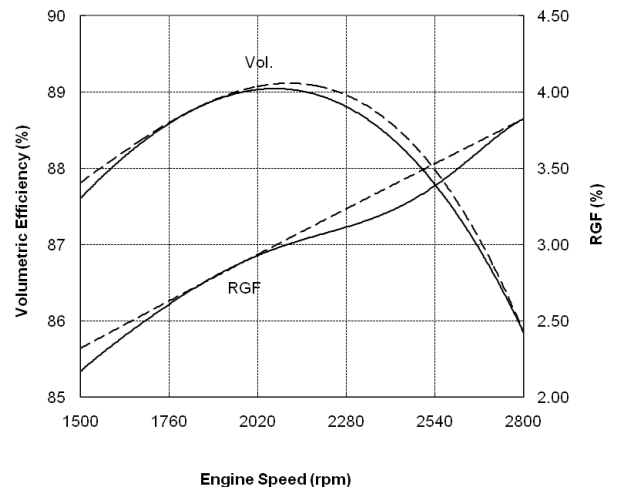

Figure 11 Volumetric efficiency and RGF vs. speed for constant and variable compression ratio engines

Figure 10 shows a significant decrease in delay period over engine speed ranged from 1500 to 2460 rpm with values between 15.3 % (0.45 degrees of crank angle) at 1500 rpm, and 6.8 % (0.3 degrees of crank angle) at 2460 rpm. Figure 11 shows that volumetric efficiency is reduced by about 0.48 % at speed of 1500 rpm, and 0.25 % at 2460 rpm passing through zero % at both 1900 and

The effect of optimal variation of compression ratio for maximum brake torque on soot and NO_x emission is shown in Figure 12. The soot emission from engine with variable compression ratio is less than that of the

conventional engine by about 9.7 % at 1500 rpm, zero % at both 1900 and 2800 rpm , and 12 % at 2460 rpm. The formed NO_x inside variable compression ratio engine is very high compared to formed at constant compression ratio by about 21.7 % (2.65 gm/kg fuel) at 1500 rpm, 90.7 % (0.461 gm/kg fuel) at 2460 rpm, and zero % at both 1800 and 2800 rpm. This increase is due to the increase of cylinder temperature with increasing r_c.
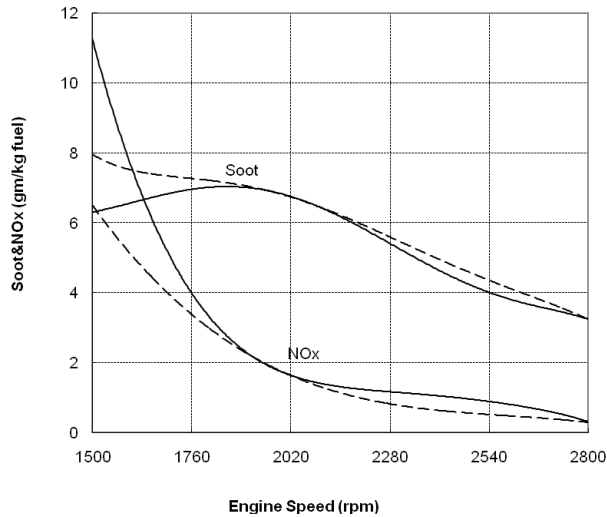

Figure 12 Soot and Nox emission vs. speed for constant and variable compression ratio engines

The conclusion based on Figs. 7-12 is that varying the compression ratio of diesel engine, within the entire range of engine speed of 1500-2800 rpm, to achieve a maximum engine torque leads to variations in the predicted performance variables compared to those predicted at constant compression ratio (r_c=16.4) . These variations can be summarized as follows: 1. at engine speed of 1500, and 2460 rpm, there is no variation in all studied variables. 2. for the other values of engine speed, the maximum pressure, maximum temperature, brake torque, thermal efficiency, and unfavorable NO_X are increasing. On the contrary, the delay period, volumetric efficiency, residual gas fraction, and soot formation are decreasing. Table-3 summarizes the predicted results of performance variables at different values of engine speed.

TABLE 2
Summary of results of varying engine compression ratio compared to those at constant compression ratio to attain constant maximum brake torque

Engine performance variables	N=1500 rpm		N=1900 rpm		N=2460 rpm	
	Increase	Decrease	Increase	Decrease	Increase	Decrease
bsfc	-	4.6 %	0	0	-	2.7 %
Max. Pressure	10.3 %	-	0	0	6 %	-
Max. Temperature	3.6 %	-	0	0	2 %	-
Brake Torque	5.4 %	-	0	0	4.6 %	-
Thermal efficiency	4.4%	-	0	0	2.8%	-
Delay Period	-	15.3 %	0	0	-	6.8 %
Vol. efficiency	-	0.48%	0	0	-	0.25%
RGF	-	6.5%	0	0	-	5%
Soot	-	9.7%	0	0	-	12%
Nox	21.7%	-	0	0	90.7%	-

CONCLUSIONS

The present investigations, which concerns a thermodynamic analysis of a four-stroke direct injection diesel engine, is based on a single-zone combustion modeling with a rapid premixed burning phase followed by a slower mixing controlled burning phase. The comparison of the numerical results with some available experimental data (under constant compression ratio), which shows a good agreement, indicate that the numerical code predicts quite reasonably the cycle performance. The numerical results showed that varying the cylinder compression ratio of moderate diesel engines led to an increase in the engine brake efficiency and power and a reduction in fuel consumption and soot emission. The increase in maximum pressure and temperature due to the optimum variation of the cylinder compression ratio are not large compared to the engine operating pressure and temperature under constant compression ratio conditions, and thus, the engine would withstand these slight increases in the maximum pressure and temperature because they are tolerable due to the safety factor. The only drawback of varying the compression ratio is the increase in NO_x, which is considerable as these increases are the maximum at specified engine speeds but beyond these speeds the NO_x emissions is low

ACKNOWLEDGMENTS

REFERENCES

[1] Roberts M. ,Benefits and challenges of variable Compression Ratio (VCR), *SAE* 2002; paper No. 03P-227
[2] Freudenstein F., Maki E.R. ,Variable-displacement piston engine, *US Patent* #4,270,495, 1981

[3]   Yamin J.A., and Dado M. H. , Performance Simulation of a Four-Stroke Engine with Variable Stroke-Length and Compression Ratio, *Appl. Energy,* vol. 77, 2004, pp. 447-463

[4]   Ladommatos N., and Balian R.A., Combustion in a Direct Injection Diesel Engine with Increased Clearance Volume, *Proc Instn Mech Engrs,* vol. 204, 1990, pp. 187-197

[5]   Rychter T.J.,   Teodorczyk A., Stone C.R., Leonard H.J., Ladommatos N., and Charlton S.J., A Theoretical Study of a Variable Compression Ratio Turbocharged Diesel Engine, *Proc Instn Mech Engrs*, vol. 206,1992, pp. 227-238

[6]   Sobotowski R.A., Potrer B.C., and Pilley A.D., The Development of Novel Variable Compression Ratio, Direct Injection Diesel Engine, *SAE 910484*

[7]   Chmela F.G. , Pirker G.H., and Wimmer A., Zero-Dimensional ROHR Simulation for DI Diesel Engines– A Generic Approach, *Energy Conversion and Management*, vol. 48, 2007, pp. 2942-2950

[8]   Arrègle   J., Lòpez J.J., Garcia J.M, and Fenollosa C., Development of a Zero-Dimensional Diesel Combustion Model. Part 1:Analysis of the Quasi-Steady Dffusion Combustion Phases, *Applied Thermal Engineering*, vol. 23, 2003, pp. 1301-1317

[9]   Kouremenous D.A., Rakopoulos C.D., and Hountalas D., Thermodynamic analysis of indirect injection diesel engine by using two-zone modeling of combustion, *Transaction of ASME, Journal of Engineering of Gas Turbine and Power*, vol. 112, 1990, pp138-149

[10] Basha S.A., and Gopal K.R., In-Cylinder Fluid Flow, Turbulence and Spray Models—a Review, *Renewable and Sustainable Energy Reviews*, vol. 13, 2009, pp. 1620–1627.

[11] Kaario O., Lendormy E., Sarjovaara T., Larmi M., and Rantanen P., In-Cylinder Flow Field of a Diesel Engine, *SAE* Paper No. 2007-01-4046.

[12] Lee C-F.F., and Zhao J., Modeling of Blowby in a Small-Bore High-Speed Direct Injection Optically Accessible Diesel Engine, *SAE* Paper No. 2006-01-0649.

[13] Han Z., and Reitz R.D., Turbulence Modeling of Internal Combustion Engines Using RNG k-ε Models, *Combustion Science and Technology*, vol. 106, 1995, pp. 267-295

[14] Hessel R.P., and Rutland C.J., Intake Flow Modeling in a Four-stroke Diesel Engine using KIVA-3, *Journal of Propulsion and Power*, vol. 11, 1995, pp. 378-384

[15] Reitz R.D., and Rutland, C.J., Development and Testing of Diesel Engine CFD Models, *Prog. Energy Sci.*, vol. 21, 1995, pp. 173-196

[16] Kopa R.D.,   Hollander B.R., Hollander F.H., and Kimura H., Combustion Temperature, Pressure and Products at Chemical Equilibrium, Report No. 64-1 Dept. of Mech. Eng., Univ. of California, 1964

[17] Bishop I.N., Effect of Design Variables on Friction and Economy, *SAE Transaction*, vol.3, 1965, pp. 334-358

[18] Heywood J.B., Modeling Combustion   and   Performance Characteristics of Internal Combustion Engines, *Proceeding of the 1976 Heat Transfer and Fluid Mechanics Institute*, 1976, pp.180-195

[19] Eichelberg G., Some New Investigations on Old Combustion-Engine Problems, *Engineering*, vol. 149, 1939, pp. 149: 463-547

[20] Rakopoulos C.D., and Hountalas D.T., Net and Gross Heat Release Rate Calculation in DI Diesel Engine Using Various Heat Transfer Models, *AES, ASME*, vol. 33, 1994

[21] Annand W.J.D ., Heat Transfer in Cylinders of Reciprocating Internal Combustion Engines, Proc. *Instn., Mech. Engrs*, vol 177, 1963, pp. 973-990

[22] Blawton B., Effect of   Compression and Expansion on Instantaneous Heat Transfer in Reciprocating Internal Combustion Engines. *Proc. Instn Mech. Engrs.,* vol. 201, 1987, 175-186

[23] Woschni G., A Universally Applicable Equation For The Instantaneous Heat Transfer Coefficient in Internal Combustion Engine, *SAE Trans*., vol. 76, 1967, pp. 3065-3083

[24] Annand, W.J.D., and TMa. H., Instantaneous Heat Transfer Rates to Cylinder Head Surface of Small Compression Ignition Engine, *Proc.Instn Mech. Engrs*., vol. 185, 1970, pp. 967-987

[25] Cheung C.G., Leung C.W., and Leung T.P., Modelling Spatial Radiative Heat Flux Distribution in a Direct Injection Diesel Engine, *Proc Instn Mech Engrs.*, vol. 208, 1994, PP. 275-283

[26] Ogurt T., Takeda A.,   Torii K., and Inaba S., Radiation Heat Transfer of Combustion Flames in a Diesel Engine, *Bulletin JSME*, vol 28, 1985, pp. 638-646

[27] Campbell A. S., *Thermodynamic analysis of combustion engines*. John Willy & Sons Press 1979

[28] Heywood J.B., *Internal Combustion Engine Fundamentals*. McGraw-Hill Science/Engineering, First Edition, 1988

[29] Ramos J.L., *Internal Combustion Engine Modeling*. Taylor & Francis; First edition, 1989

[30] Zelenik F.J., "Combustion Modeling in Internal Combustion Engines, *Combustion Science and Technology*, vol. 12, 1976, pp. 159-164

[31] Gu F., and Ball A. D., Diesel Injector Dynamic Modelling and Estimation of Injection Parameters from Impact Response. Part 1: Modelling and Analysis of Injector Impacts, *Proc Instn Mech Engrs*, vol. 210, 1996, pp. 293-302

[32] Watson N., Pilley A. D., and Marzouk M. A., Combustion Correlation for Diesel Engine simulation, *SAE* paper 1980-800029,

[33] Mehta P.S., Singal S.K., and Pundir B.P., A Comprehensive Simulation Model for Mixing and Combustion Characteristics of Small Direct Injection Diesel Engine,   *Proc Instn Mech Engrs*, vol 209, 1995, pp. 117-126

[34] Rossini F.D., Pitzer K.S., Arnett R.L., Braun R.M., and Primentel G. C., *Selected values of physical and thermodynamic properties of hydrocarbons and related compounds*. Carnegie Press., Pittsburgh, Pa, USA, 1953

[35] Hiroyasu H., and Kadota T., Models of Combustion and Formation of Nitric Oxide and Soot in DI Diesel Engine, *SAE* paper 1976-760129

[36] Morel T., and Keribar R., Heat Radiation in DI Diesel Engine, *SAE* paper 1986-860445

[37] Wahiduzzaman S., Morel T., Timar J., and De Witte D.P. , Experimental and Analysis Study of Heat Radiation in a Diesel Engine, *SAE* paper 1987-870571

[38] Han Z., Uludogan A., Hampson G.J., and Reitz R.D., Mechanism of Soot and NO_x Emission Reduction Using Multiple-Injection in a Diesel Engine, *SAE* paper 1996- 960633